Supplementary Material

Evolution of embryo implantation was enabled by the origin of decidual cells in eutherian mammals

Arun R. Chavan, Oliver W. Griffith, Daniel Stadtmauer, Jamie Maziarz, Mihaela Pavlicev, Ruth Fishman, Lee Koren, Roberto Romero, Günter P. Wagner

Supplementary Results

Decidual stromal cells in armadillo

Decidual stromal cells originated before the common ancestor of eutherians, but were secondarily lost in some eutherian lineages, particularly in those that also lost invasive placentation, such as pig, cow, horse, etc (Wildman, Chen et al. 2006, Elliot and Crespi 2009). Placentation is invasive in armadillo (Enders 1960, Chavan and Wagner 2016), but literature on the presence of DSC is equivocal (Chavan, Bhullar et al. 2016). Before investigating whether DSC have any role in suppressing IL17A, we decided to test whether DSC are present in armadillo, since this is one of the species that was used in drawing the inference that IL17A is suppressed in eutherian mammals.

Functional cooperation between transcription factors HOXA11 and FOXO1, which evolved in eutherian stem lineage, is necessary for decidual gene expression (Lynch, Brayer et al. 2009). While both of these genes are expressed in endometrial stromal fibroblasts, during decidualization, they are colocalized in the nucleus. Using immunohistochemistry, we show that HOXA11 and FOXO1 colocalize to the nucleus in the endometrial stromal cells of armadillo uterus during the peri–implantation period, and these cells histologically appear like decidual cells, i.e. they are more globular than fibroblastic, and the cells that show nuclear colocalization of HOXA11 and FOXO1 also have nuclei that look distinct from other, likely immune, cells in the endometrium (**Supp. Figure 1**).

HOXA11 and FOXO1 antibodies that cross-reacted with armadillo samples were both raised in the same host species, so we could not double-stain them in the same sections. To circumvent this problem, 2µm thin sections were made, and two adjacent sections were used for staining the two antigens separately — in 2µm sections, the same nucleus is likely to be sampled in two adjacent sections — and their colocalization was assessed by staining in corresponding nuclei on the two sections.

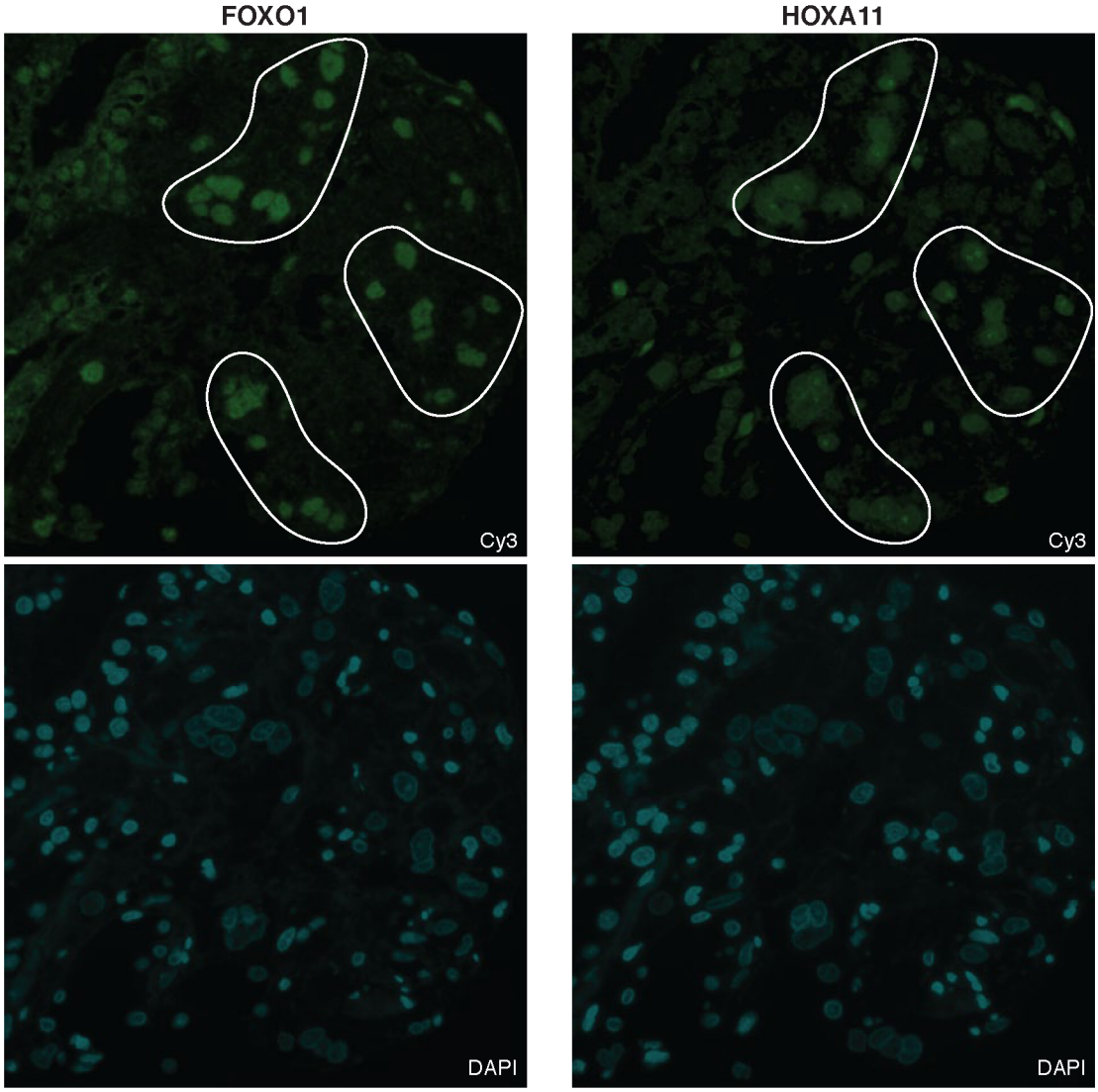

Supp. Figure 1 Decidual cells in armadillo. Immunohistochemistry for HOXA11 and FOXO1 in the endometrium of pregnant armadillo. Immunohistochemistry was done on adjacent 2µm sections. Some of the corresponding nuclei between the two sections in which HOXA11 and FOXO1 are co-expressed are outlined. These are likely decidual cells. Counterstaining is done with DAPI. Images of the two sections were aligned using image registration function in Fiji (Schindelin, Arganda-Carreras et al. 2012).

Effect of DSC conditioned medium on Th17 differentiation

Supp. Figure 2 shows the mRNA levels of *IL17A* in naïve T cells differentiated into Th17 cells with or without DSC-conditioned medium. These are the same conditions as shown in **Figure 4** (main text). mRNA abundance was measured by qPCR with $\Delta\Delta C_T$ method using TaqMan Fast Universal PCR Master Mix (4352042, Life Technologies) on StepOne Plus Real Time PCR System (Applied Biosystem). Unstimulated T cells (condition 1) were used as the

control and *TBP* gene was used as the endogenous reference. The following TaqMan probes were used: human *IL17A* (Hs00174383_m1, Thermo Fisher) and human *TBP* (4333769F, Thermo Fisher). At the mRNA level, the unconditioned DSC medium has an effect on the expression of *IL17A*, however this effect is not manifested at the secreted protein level (measured by ELISA; see main text), suggesting translational compensation. However, conditioned DSC medium has a strong effect on the *IL17A* mRNA levels as well as the secreted protein levels. This is consistent with the findings that DSC-conditioned medium suppresses the translational and secretory machinery in T cells, thereby likely suppressing their differentiation into Th17 cells.

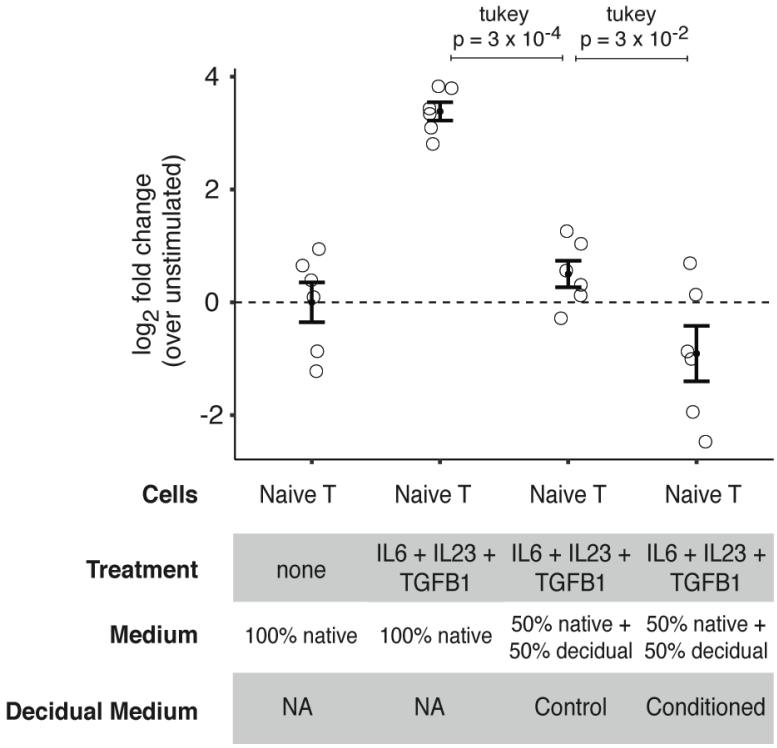

Supp. Figure 2 *IL17A* mRNA levels in T cells treated with DSC control and conditioned medium. Log_2 fold change is shown with respect to the unstimulated cells (first condition). Error bars are standard errors, and p-values shown are from Tukey test.

Potential ligand-receptor interactions between DSC and naïve T cells

To identify potential signals from DSC that suppress Th17 differentiation, we created a map of receptors expressed on naïve T cells and their cognate ligands, or enzymes that produce non-protein ligands, expressed in DSC (**Supp. Figure 3**). We produced this map from transcriptomic data of DSC and naïve T cells (see **Supp. Table 3**) using a ligand-receptor interaction dataset compiled by Pavlicev and colleagues (Pavlicev, Wagner et al. 2017). There are 29 ligands expressed in DSC for which a receptor is expressed on naïve T cells — one or more of these signals are likely to be responsible for the suppression of Th17 differentiation.

Of these, JAG1, EFNA4, EFNA5, EFNB1 can be discounted as potential candidates since they rely on cell-cell contact for ligand-receptor interaction, while the causative DSC ligands must be secreted since their effect can be seen with conditioned medium. The DSC signal could be one or more secreted molecules, potentially from the following: CXCL12, LTA4H, SST, WNT2, WNT3, WNT5A, sphingosine-1-phosphate (produced by ASAH1 and ACER3), prostaglandins (produced by PTGES2, PTGES3, and PTGDS), IL15, IGF1, IGF2, FGF1, FGF2, FGF5, FGF9, VEGFC, CTF1, TGFB1, TGFB3, BMP2, and INHBA. Of these, many molecules are known regulators of T cell differentiation and trafficking. The CXCL12/CXCR4 axis maintains the Th2 bias in cytokine profile at the fetal-maternal interface (Piao, Tao et al. 2012), IL15 downregulates IL17A expression in Th17 (Pandiyan, Yang et al. 2012) and also changes the balance of Th17 and T-reg in favour of T-reg (Tosiek, Fiette et al. 2016). Assuming that the relevant signaling molecules are induced only upon decidualization (i.e. not expressed in ESF), and are expressed in armadillo and rabbit uterus at the time of implantation, the set of candidate molecules reduces to CXCL12, WNT5A, sphingosine-1-phosphate, prostaglandins, and IL15.

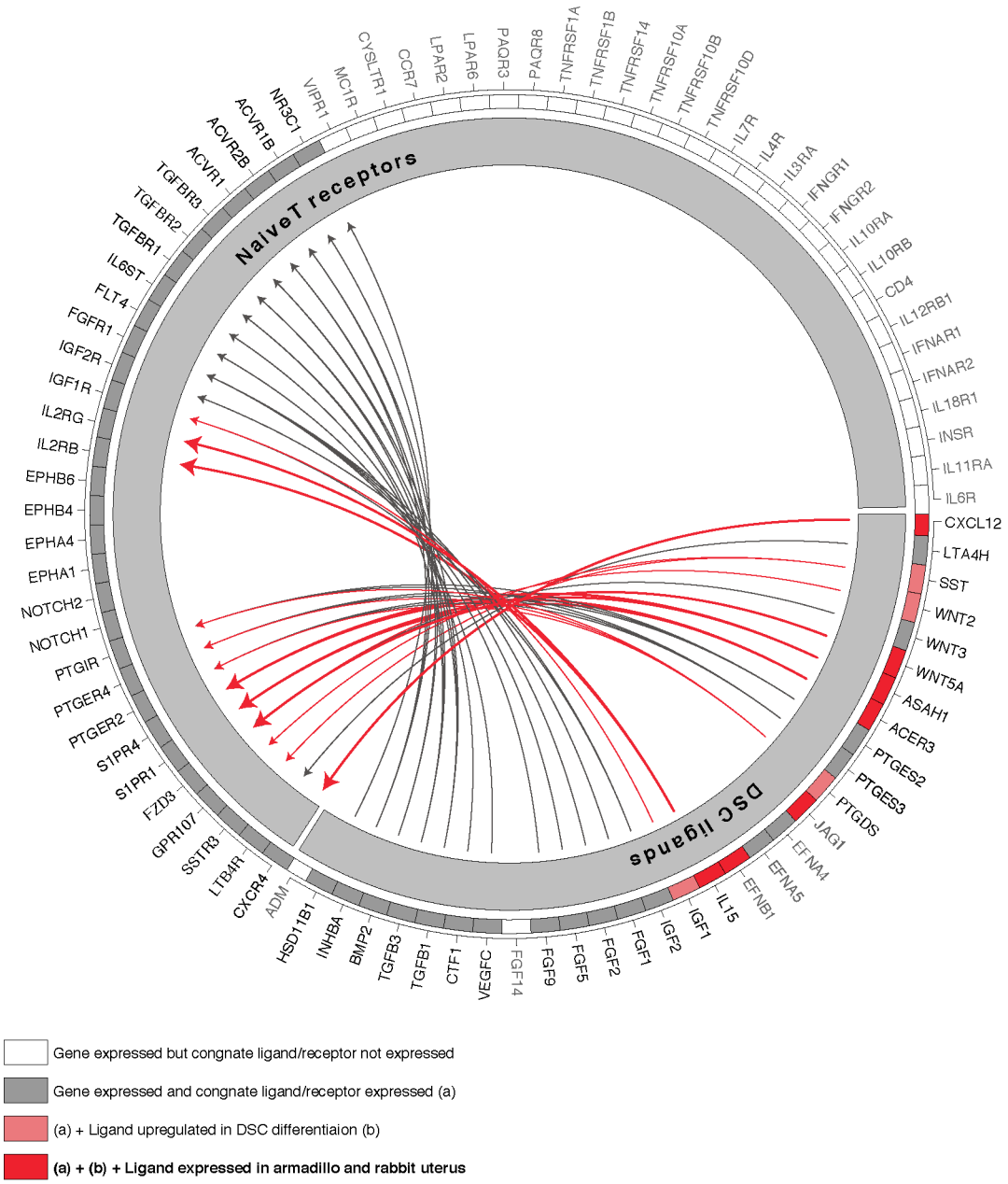

Supp. Figure 3 Ligand-receptor interactions between DSC and naïve T cells. This figure shows the map of potential signaling interactions between DSC and naïve T cells, represented in terms of ligands secreted by DSC and the receptors expressed by naïve T cells. Only the ligands and receptors that are expressed over 3 TPM are shown. White rectangles represent ligands or receptors for which the cognate molecule is not expressed in the other cell type. Grey rectangles are genes for which the cognate ligand or receptor is expressed on the other cell type — subset of these that are upregualted in DSC during decidualization are shown in light red, while those that are, in addition, also expressed in armadillo and rabbit uterus at implantation are shown in red. Arrows emanating from JAG1, EFNA1, EFNA4, and EFNB1 are removed because these molecules require cell-cell contact, whereas DSC conditioned medium is sufficient to bring about the suppression of Th17 differentiation.

Supplementary Tables

Supp. Table 1 Animals used in this study

Species	Animal ID	Stage of Pregnancy
D. novemcinctus	YPM0589	Non-pregnant
D. novemcinctus	YPM0583	Peri-implantation
P. capensis	pcap03	Peri-implantation
M. domestica	14L4	Non-pregnant
M. domestica	14L5	Non-pregnant
M. domestica	14M8	Non-pregnant
M. domestica	14M4	8 dpc
M. domestica	14M5	8 dpc
M. domestica	14M9	8 dpc
M. domestica	15P7	11.5 dpc
M. domestica	16S1	11.5 dpc
M. domestica	15P8	12.5 dpc
M. domestica	16S2	12.5 dpc
M. domestica	14N7	13.5 dpc
M. domestica	M1LT	13.5 dpc
M. domestica	17Z3	14 dpc

Supp. Table 2 Antibodies used in this study

Product ID	Company	Antigen	Host species	Immunogen species	Label	Dilution used
sc9809	Santa Cruz	FOXO1	Goat	Human	None	1:4000
sc48542	Santa Cruz	HOXA11	Goat	Human	None	1:8000
sc32294	Santa Cruz	IL1B	Mouse	Human	None	1:100
M3210	Spring	PTGS2	Rabbit	Human	None	1:1000
NB110-39058	Novus	PTGES	Rabbit	Human	None	1:100
sc2005	Santa Cruz	Mouse-IgG	Goat	Mouse	HRP	1:200
K4011	DAKO	Rabbit-IgG	Goat	Rabbit	Polymer-HRP	undiluted
sc2056	Santa Cruz	Goat-IgG	Donkey	Goat	HRP	1:200

Supp. Table 3 RNA-seq data used in this study

Species	Tissue/Cell type	Source	GEO/SRA accession	Sequencing platform
Armadillo	Uterus	This study	GSE120510	Illumina HiSeq 2500
Rabbit	Uterus	(Liu, Zhao et al. 2016)	GSE76115	Illumina HiSeq 2500
Opossum	Uterus	(Griffith, Chavan et al. 2017)	SRP111668	Illumina HiSeq 2500
Human	ESF and DSC	(Kin, Nnamani et al. 2015)	GSE63733	Illumina Genome Analyzer II
Human	Naïve T cells	(Hertweck, Evans et al. 2016)	GSE62483	Illumina HiSeq 2000
Human	Th17 cells	This study	GSE120380	Illumina HiSeq 4000

Supp. Table 4 qPCR primers

Gene		Primer (5' – 3')
IL17A (*M. domestica*)	Forward	TCTTCTCCAAGCAACTTGCCA
	Reverse	AGAGCGGTTCTTGTAATCGGG
TBP (*M. domestica*)	Forward	CTCTTCCATTCACAGACTCTTACC
	Reverse	TCAAGTTTACAACCAAGATTCACG

Supplementary files

1. HTseq read counts of gene expression: Opossum non-pregnant and 13.5 dpc (**read-counts_mdom_uterus.csv**)
2. HTseq read counts of gene expression: Rabbit implantation stage (**read-counts_ocun_uterus.csv**)
3. HTseq read counts of gene expression: Armadillo non-pregnant and implantation stage (**read-counts_dnov_uterus.csv**)
4. HTseq read counts of gene expression: Human naïve T cells treated with control and conditioned DSC medium; protein coding genes (**read-counts_hsap_tcells_protein-coding.csv**)
5. Feature lengths used for calculating TPM: Opossum (**feature-lengths_mdom.csv**)

6. Feature lengths used for calculating TPM: Rabbit (**feature-lengths_ocun.csv**)
7. Feature lengths used for calculating TPM: Armadillo (**feature-lengths_dnov.csv**)
8. 1-to-1 orthologous gene set for opossum, rabbit, and armadillo downloaded from Biomart (**one-to-one-orthologs_mdom-ocun-dnov.csv**)

Supplementary References

Chavan, A. R., B.-A. S. Bhullar and G. P. Wagner (2016). "What was the ancestral function of decidual stromal cells? A model for the evolution of eutherian pregnancy." Placenta **40**: 40-51.

Chavan, A. R. and G. P. Wagner (2016). "The fetal-maternal interface of the nine-banded armadillo: endothelial cells of maternal sinus are partially replaced by trophoblast." Zoological Letters **2**(1): 11.

Elliot, M. G. and B. J. Crespi (2009). "Phylogenetic evidence for early hemochorial placentation in eutheria." Placenta **30**(11): 949-967.

Enders, A. C. (1960). "Development and structure of the villous haemochorial placenta of the nine-banded armadillo (Dasypus novemcinctus)." Journal of Anatomy **94**(Pt 1): 34-45.

Griffith, O. W., A. R. Chavan, S. Protopapas, J. Maziarz, R. Romero and G. P. Wagner (2017). "Embryo implantation evolved from an ancestral inflammatory attachment reaction." Proceedings of the National Academy of Sciences **doi: 10.1073/pnas.1701129114**.

Hertweck, A., Catherine M. Evans, M. Eskandarpour, Jonathan C. Lau, K. Oleinika, I. Jackson, A. Kelly, J. Ambrose, P. Adamson, David J. Cousins, P. Lavender, Virginia L. Calder, Graham M. Lord and Richard G. Jenner (2016). "T-bet Activates Th1 Genes through Mediator and the Super Elongation Complex." Cell Reports **15**(12): 2756-2770.

Kin, K., Mauris C. Nnamani, Vincent J. Lynch, E. Michaelides and Günter P. Wagner (2015). "Cell-type Phylogenetics and the Origin of Endometrial Stromal Cells." Cell Reports **10**(8): 1398-1409.

Liu, J.-L., M. Zhao, Y. Peng and Y.-S. Fu (2016). "Identification of gene expression changes in rabbit uterus during embryo implantation." Genomics **107**(5): 216-221.

Lynch, V. J., K. Brayer, B. Gellersen and G. P. Wagner (2009). "HoxA-11 and FOXO1A cooperate to regulate decidual prolactin expression: towards inferring the core transcriptional regulators of decidual genes." PLoS One **4**(9): e6845.

Pandiyan, P., X.-P. Yang, S. S. Saravanamuthu, L. Zheng, S. Ishihara, J. J. O'Shea and M. J. Lenardo (2012). "The Role of IL-15 in Activating STAT5 and Fine-Tuning IL-17A Production in CD4 T Lymphocytes." The Journal of Immunology **189**(9): 4237.

Pavlicev, M., G. P. Wagner, A. R. Chavan, K. Owens, J. Maziarz, C. Dunn-Fletcher, S. G. Kallapur, L. Muglia and H. Jones (2017). "Single-cell transcriptomics of the human placenta: inferring the cell communication network of the maternal-fetal interface." Genome Res **27**(3): 349-361.

Piao, H.-L., Y. Tao, R. Zhu, S.-C. Wang, C.-L. Tang, Q. Fu, M.-R. Du and D.-J. Li (2012). "The CXCL12/CXCR4 axis is involved in the maintenance of Th2 bias at the maternal/fetal interface in early human pregnancy." Cellular And Molecular Immunology **9**: 423.

Schindelin, J., I. Arganda-Carreras, E. Frise, V. Kaynig, M. Longair, T. Pietzsch, S. Preibisch, C. Rueden, S. Saalfeld, B. Schmid, J.-Y. Tinevez, D. J. White, V. Hartenstein, K. Eliceiri, P. Tomancak and A. Cardona (2012). "Fiji: an open-source platform for biological-image analysis." Nat Meth **9**(7): 676-682.

Tosiek, M. J., L. Fiette, S. El Daker, G. Eberl and A. A. Freitas (2016). "IL-15-dependent balance between Foxp3 and RORγt expression impacts inflammatory bowel disease." Nature Communications **7**: 10888.

Wildman, D. E., C. Y. Chen, O. Erez, L. I. Grossman, M. Goodman and R. Romero (2006). "Evolution of the mammalian placenta revealed by phylogenetic analysis." Proceedings of the National Academy of Sciences of the United States of America **103**(9): 3203-3208.